NONINVASIVE STUDY OF SPATIO-TEMPORAL VARIABILITY OF B2B VENTRICULAR DEPOLARIZATION AND REPOLARIZATION

K. Haraszti*, Gy. Kozmann**

* Research Institute for Technical Physics and Materials Science / Dept. of Bioengineering,
H-1121 Konkoly-Thege Miklós u. 29-33., Budapest, Hungary
** University of Veszprém / Dept. of Information Systems,
H-8200 Egyetem u. 10., Veszprém, Hungary

haraszti@mfa.kfki.hu

Abstract: Spatial repolarization disparity is widely acknowledged as a substrate of malignant arrhythmia vulnerability e.g. [1]. Recently, the beat-to-beat (B2B) QT variability was also considered as a sign of arrhythmia vulnerability e.g. [2]. In this study the spatio-temporal action potential dynamics were assessed by the use of body surface potential map (BSPM) records. The complex spatio-temporal dynamics of ventricular depolarization and repolarization was compared on a beat-to-beat basis in normal subjects and arrhythmia patients. Records were taken with a typical length of 5 minutes. The spatio-temporal nature of activation and repolarization sequence was characterized by QRS and QRST integral and integral difference maps. Furthermore, RR distances, nondipolarity indices (NDI) and the α angle of 192D QRS and QRST vectors were used to assess depolarization and repolarization dynamics. Results revealed that repolarization changes are causally preceded by perturbations in the depolarization process. Substantial non-overlapping information was found in the frequency spectra of the heart rate (RR) parameter and in the spatial activation and repolarization complexity, represented by NDI.

Introduction

According to basic electrophysiological experiments, arrhythmia vulnerability is associated with elevated disparity of ventricular repolarization. Several possible mechanisms were studied that may result in the elevation of arrhythmia vulnerability. Noninvasive methods were recommended for the detection of pathological repolarization disparity, including measurements performed on low-noise averaged majority beats, QT dispersion estimates etc. [1], [3], [4], [5], [6] and [7]. Other approaches try to get information from the beat-to-beat lability of QT duration in ECG leads[8], time- and frequency domain heart rate variability measurements, as well as from the vulnerability changes evoked by single or multiple premature stimuli [9], [10], and [11].

In this paper the theoretically well understood QRS and QRST integral maps and scalar parameters extracted from the subsequent beats are used to characterize malignant changes in a train of beats. Now, a special attention has been paid to the variability of the beat-to-beat spatio-temporal QRS and QRST integral dynamics in sinus rhythm in health and disease.

Materials and Methods

Noninvasive spatio-temporal depolarization and repolatization dynamics was assessed by the use of long BSPM records taken on 10 young healthy male and female subjects and in 10 documented male and female IHD patients, with a typical length of 5 minutes. Map data were recorded from 64 chest positions according to the electrode layout suggested in Amsterdam by the Dutch BioSemi Mark-8 Quad (2048 Hz sample rate, 16 bit amplitude resolution, see details at [12]).

Data processing started with the identification of individual beats, high-precision determination of QRS fiducial points, and classification of beat patterns according to their QRS shape. Subsequently, Q_{on}, S_{end} and T_{end} points were marked in each majority group heart cycle by an automatic procedure, but the final position of these points was adjusted by human intervention. For premature beats, when R waves were superimposed on the previous T waves, a special subtraction algorithm was applied for the separation of waves, similar to that discussed in [13]. After a linear base-line adjustment from the measured 64 signals, unipolar ECG signals were estimated in 128 un-measured chest locations of the 192-lead arrangement introduced at the CVRTI, Salt Lake City. The procedure of signal estimations followed the principle suggested by [14], (1).

$$\begin{bmatrix} \phi_{m1} \\ \vdots \\ \vdots \\ \vdots \\ \vdots \\ \phi_{m192} \end{bmatrix} \cong \begin{bmatrix} \phi_{m1} \\ \vdots \\ \phi_{m64} \\ \phi_{e1} \\ \vdots \\ \phi_{e128} \end{bmatrix} = \begin{bmatrix} \bar{\phi}_{measured} \\ \bar{\phi}_{estimated} \end{bmatrix} = \begin{bmatrix} \bar{\phi}_{measured} \\ \overline{T} \times \bar{\phi}_{measured} \end{bmatrix} \qquad (1)$$

ISSN: 1727-1983

where ϕ_{mi} and ϕ_{ei} are the measured and estimated potential in the i^{th} point of the body surface, $\overline{\overline{T}} = \left[\overline{\overline{K}}'_{12} \times \overline{\overline{K}}^{-1}_{11} \right]$ and K_{12} and K_{11} are minor matrices of the 192D covariance matrix.

Finally QRS and QRST integrals were computed from the data of the 192-lead system (2), (3):

$$\int_{QRS} \phi(P,t)dt = -\iint_{S} \mathbf{z}(P,\mathbf{r})\boldsymbol{\tau}(\mathbf{r})dF_S \qquad (2)$$

where $\phi(P,t)$ is the potential in the P point of the body surface at the moment t, $\mathbf{z}(P,\mathbf{r})$ is the vector of the transfer coefficients between a point of the surface of the heart and the P point of the body surface, $\boldsymbol{\tau}(\mathbf{r})$ is the activation sequence of the epi- endocardial surface and $\mathbf{S}_\tau(\mathbf{r})$ is the source vector in $\mathbf{r}$; S is the endo-epicardial surface

$$\int_{QRST} \phi(P,t)dt = -k\iiint_{V_S} \mathbf{z}(P,\mathbf{r})\nabla\mu(\mathbf{r})dV_S \qquad (3)$$

where $\phi(P,t)$ is the potential in the P point of the body surface at the moment t, $\mathbf{z}(P,\mathbf{r})$ is the vector of the transfer coefficients between a point of the surface of the heart and the P point of the body surface and $\nabla\mu$ is the ventricular gradient, Vs is the myocardial volume.

For the detailed quantitative representation of beat-by-beat spatial activation and repolarization patterns, QRS and QRST integral maps and difference maps (indicating departure from the average distributions) were drawn. The temporal dynamics in cycle length was assessed by the time series of RR distances and the angle spanned by the 192D QRS and QRST vectors. Depolarization and repolarization dinamics were characterized by the Karhunen-Loève (KL) expansion parameters of QRS and QRST integral maps, respectively and by the non-dipolarity index (NDI) introduced at the CVRTI, Salt Lake City.

RR, KL, and NDI time-series were systematically analyzed both in the time and frequency domain, by the STATISTICA program package (auto-, and cross correlation, spectral density, coherence, etc.)

Results

Individual QRS and QRST integral maps of healthy subjects show a stable overall pattern along the time coordinate. The relevant Box and Whiskers plot reveal no significant scattering in the KL data (Fig. 1 upper graph) QRST integral map SD^2/M^2 (amplitude variance/mean signal energy) amplitude values ranged in our sample group between 0.0057-0.008, the values for the QRS integral variability were similar. The spatial pattern of the beat-to-beat integral map differences was random in both integral maps.

In the group of ARR patients both the QRS and QRST integral map variability amplitudes increased significantly compared to the healthy group, while the random character of the pattern changes persisted (Fig.1 lower graph). The QRST integral amplitude SD^2/M^2 values went up to 0.021-0.069.

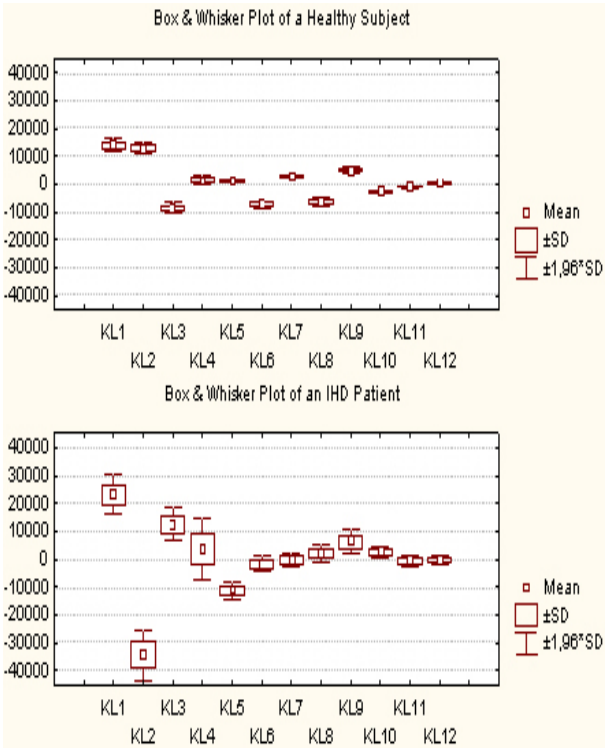

Figure 1: Box and Whisker diagrams of the QRST integral KL coefficient variability of a healthy subject (upper) and an IHD patient (lower).

Correlation matrices of the simultaneously measured KL coefficients (representing the spatial pattern of the individual QRST integral maps) did show marked linear relationships between certain coefficients, especially in normal subjects, see Table 1.

Table 1: Correlation matrices of QRST integral map coefficients. (Only the first 6 KL coefficient correlations are printed of the patients shown in Fig. 1.)

	KL1	KL2	KL3	KL4	KL5	KL6
KL1	1,00	0,27	-0,07	-0,35	0,14	-0,23
KL2	0,27	1,00	-0,76	0,10	0,59	-0,72
KL3	-0,07	-0,76	1,00	-0,06	-0,48	0,69
KL4	-0,35	0,10	-0,06	1,00	-0,25	-0,23
KL5	0,14	0,59	-0,48	-0,25	1,00	-0,28
KL6	-0,23	-0,72	0,69	-0,23	-0,28	1,00

	KL1	KL2	KL3	KL4	KL5	KL6
KL1	1,00	0,27	0,22	0,02	0,10	0,12
KL2	0,27	1,00	-0,03	0,21	0,49	0,13
KL3	0,22	-0,03	1,00	0,25	0,00	0,07
KL4	0,02	0,21	0,25	1,00	-0,18	0,06
KL5	0,10	0,49	0,00	-0,18	1,00	-0,02
KL6	0,12	0,13	0,07	0,06	-0,02	1,00

ISSN: 1727-1983

The correlation matrices of healthy subjects did show significant linear relationship between certain coefficients, but in patients the correlations had a diminishing tendency, suggesting almost independent random fluctuations both in the QRS and QRST integral KL coefficients.

Autocorrelation functions each of the KL time-series exhibited a (respiration related) periodicity in most of our healthy subjects, but almost a white-noise pattern was found in ARR patients, see Fig. 2.

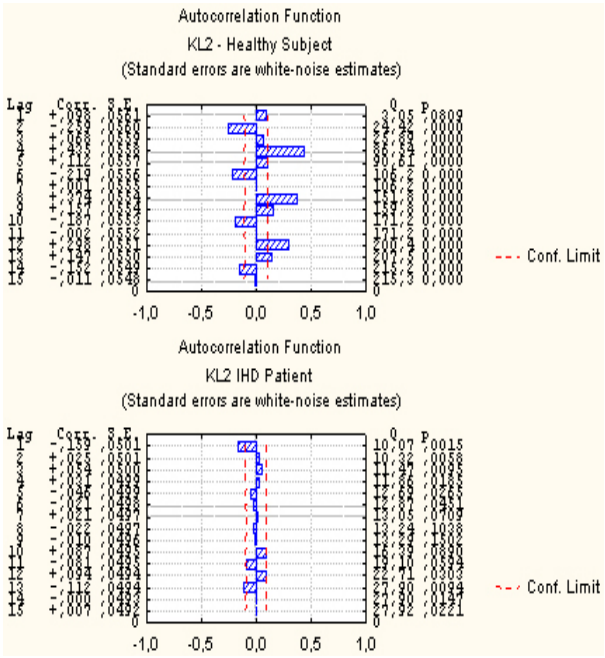

Figure 2: Autocorrelation functions of the 2nd KL coefficients for the same patients as in Fig. 1.

In normal subjects the autocorrelation functions of the KL components revealed a respiration dependent integral map pattern modulation. The pattern modulation partly may be due to the passive, respiration dependent quasi-periodic rotation and translation of the heart and also due to the neural volume control. In IHD cases, the autocorrelation functions of each KL coefficient time-series did show a white-noise like pattern, the modulation due to respiration was hardly recognizable. In this case the time-domain signs of sinus arrhythmia significantly diminished, the respiration dependent peak in the power spectral density was significantly reduced. However, the noise-like frequency components above the respiration frequency significantly increased, see Fig. 3.

The association of the QRS and QRST integrals was studied by a multiple regression model comprising the KL components of the beat-by-beat deviations in both integral maps. In the examples studied the general regression models provided multiple R values in the range of (0.73-0.93), while the relevant multiple R^2 values ranged from 0.66 to 0.88.

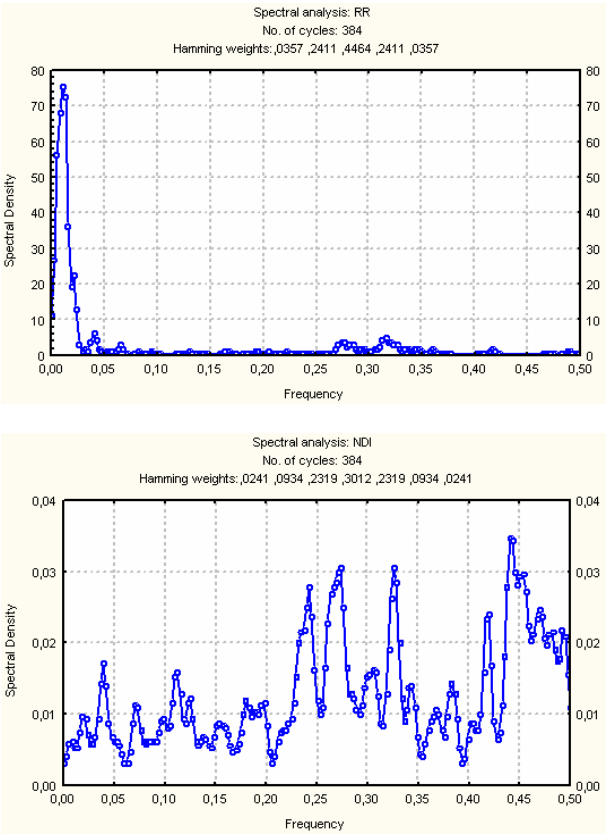

Figure. 3: Example on the IND power spectral density in health and in IHD.

Discussion

Based on theoretical assumptions QRS integral maps provide the body surface projection of the ventricular activation sequence, while QRST integral maps visualize the surface projection of the ventricular gradient [3, 4]. In both cases the source level information is weighted by the very same lead field. Consequently the dynamics of QRS and QRST integral maps are directly related to the underlying beat-to-beat depolarization and repolarization variability.

Our results suggest that the baroreflex control in healthy subjects happens in a harmonic way by the modulation of heart frequency and by the distributed control of the myocardial contractility. In IHD patients the baroreflex heart-rate control is significantly compromised. The associated volume control is getting fragmented which is manifested in the elevated spatial disparity of depolarization and repolarization. According to our previous findings the level of repolarization disparity in terms of the index of nondipolarity (IND) has significant beat-to-beat variability [15].

R and R^2 values of the KL components of the QRST integral maps based on the components of the QRS integral maps reveals that the phenomena of depolarization and repolarization variability is closely associated on a cellular basis, but the relationship is not simply linear i.e. both the action potential duration and shape is a subject of beat-to-beat changes.

ISSN: 1727-1983

Conclusions

Simultaneous evaluation of QRS and QRST integral maps provide an insight in the complex modulation of ventricular depolarization and repolarization. According to our preliminary findings, map-type studies, offer an unexplored source of information in the study of arrhythmia vulnerability.

Acknowledgements

This study was supported by the National Research Found grants NKFP 2/052/2001 and OTKA F035268 of the Ministry of Education, Hungary.

References

[1] HUBLEY-KOZEY C. L., MITCHELL L. B., GARDNER M. J., WARREN J. W., PENNEY C. J., SMITH E. R., HORACEK B. M. (1995): 'Spatial Features in Body-Surface Potential Maps Can Identify Patients with a History of Sustained Ventricular Tachycardia', *Circulation*, **92(7),** pp. 1825-1838.

[2] HAIGNEY M. C., ZAREBA W., GENTLESK P. J., GOLDSTEIN R. E., ILLOVSKY M., MCNITT S., ANDREWS M. L., MOSS A. J.; MULTICENTER AUTOMATIC DEFIBRILLATOR IMPLANTATION TRIAL II INVESTIGATORS. (2004): 'QT Interval Variability and Spontaneous Ventricular Tachycardia or Fibrillation in the Multicenter Automatic Defibrillator Implantation Trial (MADIT) II Patients', *J Am Coll Cardiol.,* **44(7),** pp. 1481-1487.

[3] DE AMBROGGI L., AIME E., CERIOTTI C., ROVIDA M., NEGRONI S. (1997): 'Mapping of Ventricular Repolarization Potentials in Patients with Arrhythmogenic Right Ventricular Dysplasia: Principal Component Analysis of the ST-T Waves', *Circulation*, **96(12)**, pp. 4314-4318

[4] NADEAU R., ACKAOUI A., GIORGI C., SAVARD P., SHENASA M., PAGE P. (1988): 'PQRST Isoarea Maps from Patients with the WPW Syndrome: an Index for Global Alterations of Ventricular Repolarization', *Circulation*, **77(3),** pp. 499-503

[5] LOMBARDI F. (2000): 'Chaos Theory, Heart Rate Variability, and Arrhythmic Mortality', *Circulation*, **101(1),** pp. 8-10

[6] MITCHELL L. B., HUBLEY-KOZEY C. L., SMITH E. R., WYSE D. G., DUFF H. J., GILLIS A. M., HORACEK B. M. (1992): 'Electrocardiographic Body Surface Mapping in Patients with Ventricular Tachycardia. Assessment of Utility in the Identification of Effective Pharmacological Therapy.' *Circulation*, **86(2),** pp. 383-393

[7] SURAWICZ B. (1996): 'Will QT Dispersion Play a Role in Clinical Decision-Making?' *J Cardiovasc Electrophysiol*, **7(8)**, pp. 777-784

[8] BERGER R. D., KASPER E. K., BAUGHMAN K. L., MARBAN E., CALKINS H., TOMASELI G. F. (1997): 'Beat-to-Beat QT Interval Variability. Novel Evidence for Repolarization Lability in Ischemic and Nonischemic Dilated Cardiomyophaty.' *Circulation*, **96,** pp. 1557-1565

[9] LAURITA K. R., GIROUARD S. D., ROSENBAUM D. S. (1996): 'Modulation of Ventricular Repolarization by a Premature Stimulus', *Circ Res*, **79(3),** pp. 493-503

[10] LAURITA K. R., GIROUARD S. D., AKAR F. G., ROSENBAUM D. S. (1998): 'Modulated Dispersion Explains Changes in Arrhythmia Vulnerability during Premature Stimulation of the Heart', *Circulation*, **98(24),** pp. 2774-2780

[11] SHIMIZU S., KOBAYASHI Y., MIYAUCHI Y., OHMURA K., ATARASHI H., TAKANO T. (2000): 'Temporal and Spatial Dispersion of Repolarization during Premature Impulse Propagation in Human Intact Ventricular Muscle: Comparison between Single vs Double Premature Stimulation', *Europace*, **2(3),** pp. 201-206

[12] BIOSEMI, INTERNET SITE ADDRESS: HTTP://WWW.BIOSEMI.COM/MARK8_FULL_SPECS.HTM

[13] SIPPENSGROENEWEGEN A., MLYNASH M. D., ROITHINGER F. X., GOSEKI Y., LESH M. D. (2001): 'Electrocardiographic Analysis of Ectopic Atrial Activity Obscured by Ventricular Repolarization: P Wave Isolation Using an Automatic 62-Lead QRST Subtraction Algorithm', *J Cardiovasc Electrophysiol*, **12(7),** pp. 780-790

[14] LUX R. L., SMITH C. R., WYATT R. F., ABILDSKOV J. A. (1978): 'Limited Lead Selection for Estimation of Body Surface Potential Maps in Electrocardiography', *IEEE Trans. Biomed Eng*, **25(3),** pp. 270-276

[15] KOZMANN GY., HARASZTI K. (2004): 'Comprehensive Assessment of Cardiac Activation and Repolarization Dynamics by Body Surface Potential Mapping', *Int. J. of Bioelectromagnetism*, **6(1),** pp. xx-xx

ISSN: 1727-1983